Electronic Supplementary Information

Fluorine-free etching and ingenious constructing hydrogel layer prepared MXene membranes for oily wastewater separation

Xuan Long, Yijian Zheng, Jun Hu, Rongtong Wang, Wenjie Luo, Kai Han, Feipeng Jiao*

College of Chemistry and Chemical Engineering, Hunan Provincial Key Laboratory of Efficient and Clean Utilization of Manganese Resources, Central South University, Changsha 410083, PR China

*Corresponding author. E-mail: jiaofp@csu.edu.cn & jiaofp@163.com;

Fax: +86731 88830833; Tel: +86 731 8883083

2. Experiment

2.1. Materials

Ti_3AlC_2 MAX phase power (200 mesh, 98%) was obtained from Jili 11 Technology Co., Ltd. Sodium alginate (SA, AR) and *n*-hexane (AR, >97%) were obtained from Energy Chemical Co., Ltd. Carbon tetrachloride (CCl_4, AR) was purchased from Guangdong Guanghua Sci-Tech Co., Ltd. Kerosene (density: 0.80 g/cm^3, viscosity: 2.5 mPa·s) and cupric chloride ($CuCl_2$) were obtained from Shanghai Macklin Biochemical Co., Ltd. Hydrochloric acid (HCl, analytical grade) was purchased from Chengdu Kelong Chemical Co., Ltd. Rapeseed oil (density: 0.92 g/cm^3, viscosity: 14.0 mPa·s) was purchased from Daodaoquan Grain and Oil Co., Ltd. Potassium chloride (KCl, AR), sodium hydroxide (NaOH, AR), sodium chloride (NaCl, AR), Sudan II, and ammonium persulfate ($(NH_4)_2S_2O_8$, AR) were purchased from Shanghai Hushi Laboratorial Equipment Co., Ltd. Sodium dodecyl sulfonate (SDS, chemical pure) and tetrachloroethylene (C_2Cl_4, AR) were purchased from Xilong Scientific Co., Ltd. Commercial polyvinylidene fluoride (PVDF) membranes ((hydrophilic type, 0.45 μm in average pore size, 50 mm in diameter) were obtained from Haining Kewei Filter Equipment Co., Ltd. The extractant wastewater was supplied from Hunan Lihe Houpu technology Co., LTD.

2.2. Preparation of $Ti_3C_2Cl_2$

Similar to other molten salt methods[1], in a typical process, 1 g of the Ti_3AlC_2 MAX phase was ground homogeneously with 2.073 g of $CuCl_2$, 0.6 g of NaCl, and 0.766 g of KCl, their molar ratio (Ti_3AlC_2:$CuCl_2$:NaCl:KCl) being 1:3:2:2. Subsequently, the mixture was reacted in an Ar atmosphere at 700°C for 10 h with a warming rate of 4°C/min. After the reaction was completed, the above reactants were washed with deionized water to remove excess salt. The precipitate was

obtained by filtration and dried under vacuum at 45°C, noted as $Ti_3C_2Cl_2$-Cu. Then, the $Ti_3C_2Cl_2$-Cu powder was placed in 0.5 m of $(NH_4)_2S_2O_8$ solution (APS) and stirred for 1 h to remove Cu monomers. Finally, the precipitate was washed with deionized water, dried under vacuum at 45°C, and labeled $Ti_3C_2Cl_2$.

2.3. Preparation of $Ti_3C_2Cl_2$-$(CuSA)_5$ suspension

First, 300 mg of $Ti_3C_2Cl_2$ powder was dispersed in 0.1 mol/L $CuCl_2$ solution, thoroughly sonicated for 15 min, centrifuged, and washed once with deionized water. Similarly, the above precipitate was dispersed in 0.1 wt% SA solution, sonicated for 15 min, and centrifuged once for deionized water washing. At this point, the reaction cycle was executed once, and then four more times, for a total of five times. Afterwards, the concentration of the suspension was adjusted to 2 mg/mL, called $Ti_3C_2Cl_2$-$(CuSA)_5$. At the same time, the reaction cycles were executed 10 and 15 times, called $Ti_3C_2Cl_2$-$(CuSA)_{10}$ and $Ti_3C_2Cl_2$-$(CuSA)_{15}$, respectively.

2.4. Preparation of $Ti_3C_2Cl_2$-$(CuSA)_5$ membrane

Before preparing the membrane material, the suspension was fully sonicated. Then, 10 mL of the $Ti_3C_2Cl_2$-$(CuSA)_5$ suspension was filtered on a commercial PVDF substrate membrane, which was preserved in water and referred to as the $Ti_3C_2Cl_2$-$(CuSA)_5$ membrane. The diameter of the PVDF substrate membrane was 5 mm and the sample diameter was 3.9 mm. Moreover, the mass of the sample loaded on each membrane was calculated by weighing the mass of the PVDF substrate membrane before and after filtration. The membranes prepared from suspensions of $Ti_3C_2Cl_2$, $Ti_3C_2Cl_2$-$(CuSA)_{10}$, and $Ti_3C_2Cl_2$-$(CuSA)_{15}$ under the same conditions were called $Ti_3C_2Cl_2$, $Ti_3C_2Cl_2$-$(CuSA)_{10}$, and $Ti_3C_2Cl_2$-$(CuSA)_{15}$ membranes, respectively.

2.5. Oil-in-water emulsion separation performance

The *n*-hexane, kerosene, and rapeseed oil were used as the oil phase for oil-in-water emulsion preparation. The oil to water ratio was 1:100 and SDS was utilized as surfactant for further preparation of SDS-stabilized emulsion at 0.2 mg/mL. Subsequently, the mixture was stirred at 4000 rpm for 10 min by means of a laboratory high-speed dispersion homogenizer.

The emulsion separation performance was carried out on a laboratory-made cross-flow device[2]. The weight of the filtrate was recorded every 2 min by a computer, which in turn calculated the time permeability. The permeance F (L m^{-2} h^{-1} bar^{-1}) and separation efficiency (R) can be measured according to the following equations:

$$F = \frac{m}{\rho \times S \times \Delta t \times \Delta p} \quad (1)$$

$$R = \frac{C_0 - C_1}{C_0} \times 100\% \quad (2)$$

Where m (kg) represents the mass of the filtrate, ρ (1kg/L) represents the density of the filtrate (water), S (m^2) represents the actual filtration area, Δt (h) represents the corresponding separation time of the filtrate mass, Δp (bar) represents the extra transmembrane pressure, C_0 (mg/L) represents the oil content of the feed emulsions, and C_1 (mg/L) represents the oil content of the filtrate.

2.6. Antimicrobial performance evaluation of membrane

The membrane material was cut into 1.5×3.5 rectangles placed in petri dishes and sterilized by irradiation under UV lamp on both sides separately for 30 min. After sterilization, the membrane was transferred to a 50 mL centrifuge tube. Diluted the *E. coli* bacterial solution to 10^6 CFU/mL with LB broth medium (25 mg/mL) liquid medium and added 30 mL of the diluted bacterial solution to the centrifuge tube described above. Subsequently, the centrifuge tubes were placed in a 37 ℃ constant temperature incubator for 24 h. After the incubation was completed, the membrane was removed and placed in a new 50 mL centrifuge tube, washed with 15 mL of LB liquid medium and

the wash solution was collected. Diluted the above wash solution 10 times with sterile PBS solution. Then, 100 μL of the dilution was evenly coated on LB solid medium and placed in a constant temperature incubator at 37 ℃ for 18 h. After the incubation was completed, it was removed for photographing and recording the number of colonies. Antimicrobial resistance can be obtained by performing calculations based on *Eq. 2*.

2.7. Characterization

The scanning electron microscope (SEM, TESCAN MIRA LMS, Czech Republic) and X-ray polycrystalline powder diffractometer (XRD, Ultima IV Rigaku, Corporation) were applied to characterize the microstructures and crystal structure of the samples and membranes. Hydrogel layer around the sample was observed by the transmission electron microscope (TEM, FEI Tecnai G2 F20, USA). Optical profilometer measurement (Bruker Countor GT K 3D) was employed to characterize the surface roughness of membranes. Surface chemical compositions of samples and membranes were characterized by a Fourier transform infrared spectrometer (FT-IR, Nicolet Avatar 360 FT-IR spectrometer) and X-ray photoelectron spectrometer (XPS, Thermo Scientific K-Alpha). Underwater wettability properties were characterized by an angle measuring instrument (JC 2000D1, Zhongchen Digital Equipment Co. Ltd., China). The particle size meter (Malvern Zetasizer Nano-ZS ZEN3600), digital optical microscope (XSP-BM-30 AD, China), and infrared oil measuring instrument (HX-OIL-10, Huaxin Rui (Qingdao) Analysis Instrument Co., Ltd.) were used to characterized emulsions and filtrates.

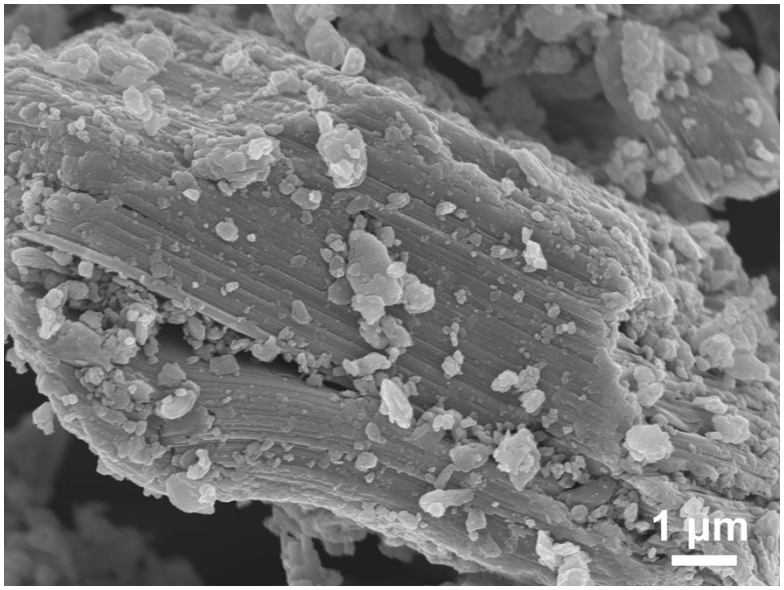

Fig. S1. SEM images of Ti_3AlC_2 MAX phase.

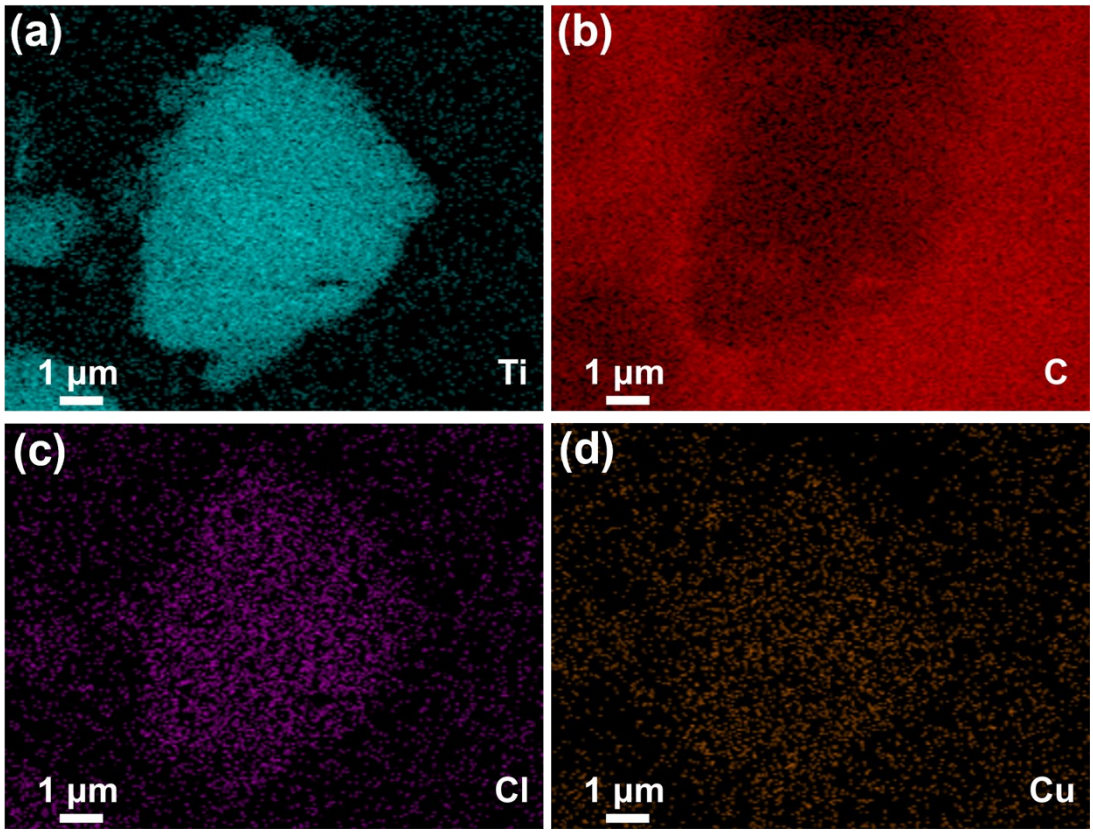

Fig. S2. EDS elemental mappings of $Ti_3C_2Cl_2$.

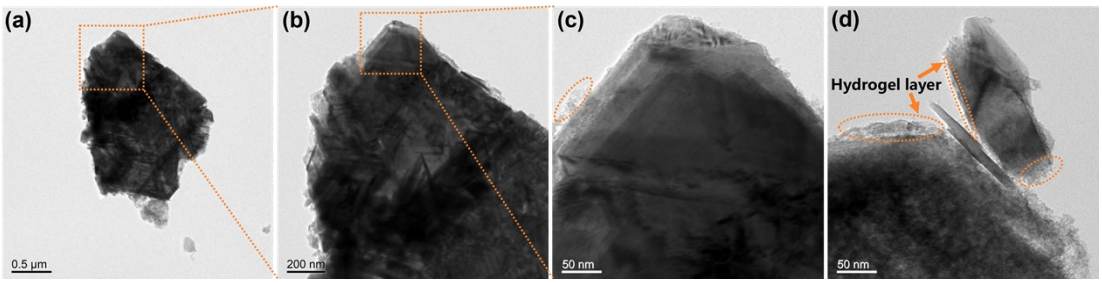

Fig. S3. (a-d) TEM images of $Ti_3C_2Cl_2$-$(CuSA)_5$.

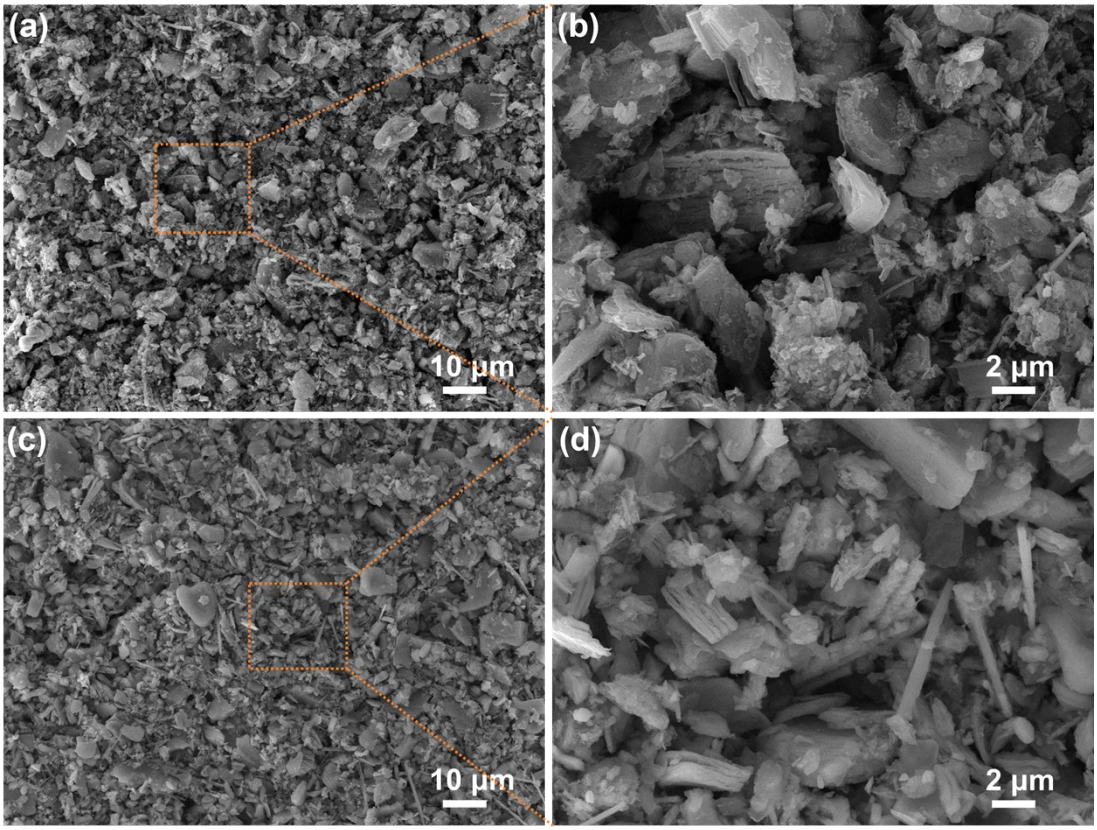

Fig. S4. SEM images of (a, b) $Ti_3C_2Cl_2$ and (c, d) $Ti_3C_2Cl_2$-$(CuSA)_5$ membranes.

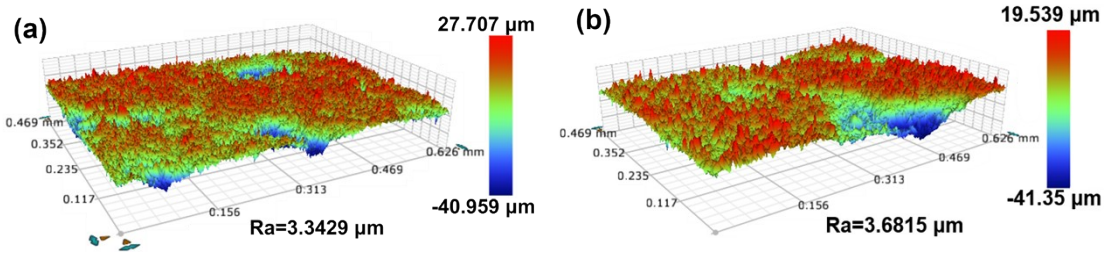

Fig. S5. 3D surface contour images of (a) $Ti_3C_2Cl_2$ and (b) $Ti_3C_2Cl_2$-$(CuSA)_5$ membranes.

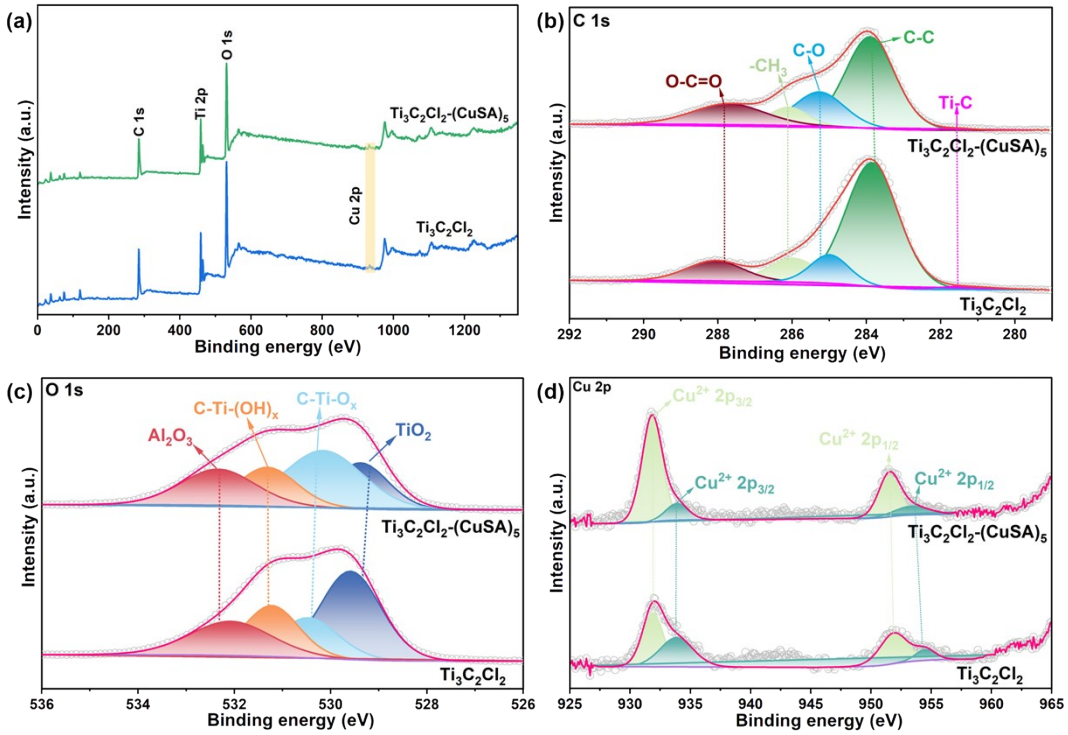

Fig. S6. (a) XPS survey spectra, (b) C 1s, (c) O 1s, and (d) Cu 2p of $Ti_3C_2Cl_2$, and $Ti_3C_2Cl_2$-$(CuSA)_5$.

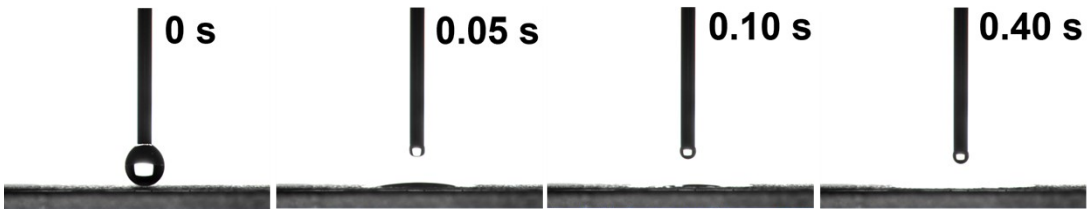

Fig. S7. Dynamic hydrophilicity images of the $Ti_3C_2Cl_2$-$(CuSA)_5$ membrane.

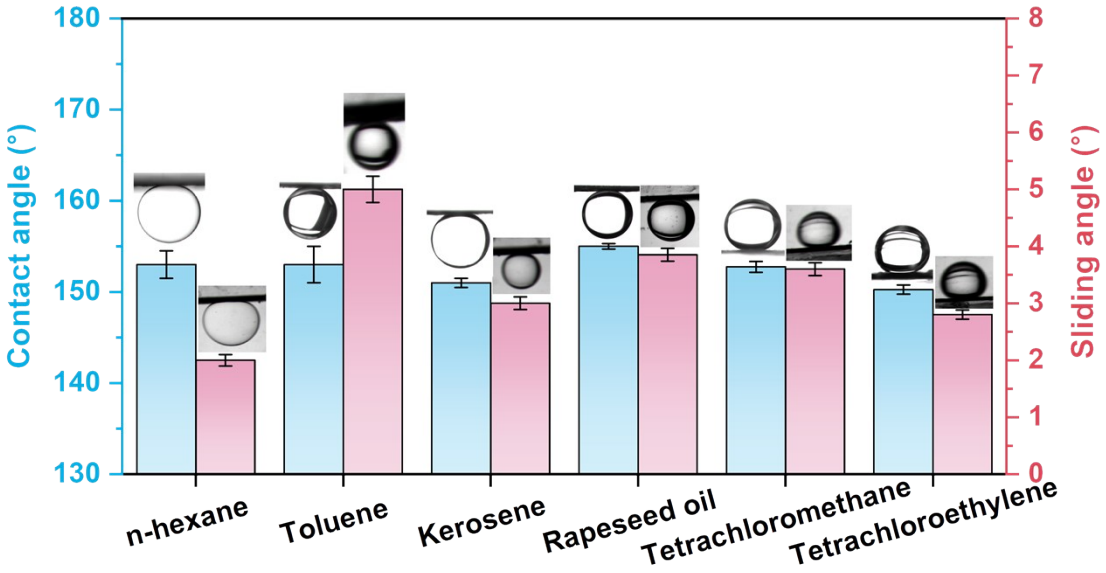

Fig. S8. Underwater oils CAs and SAs of the $Ti_3C_2Cl_2$-$(CuSA)_5$ membrane.

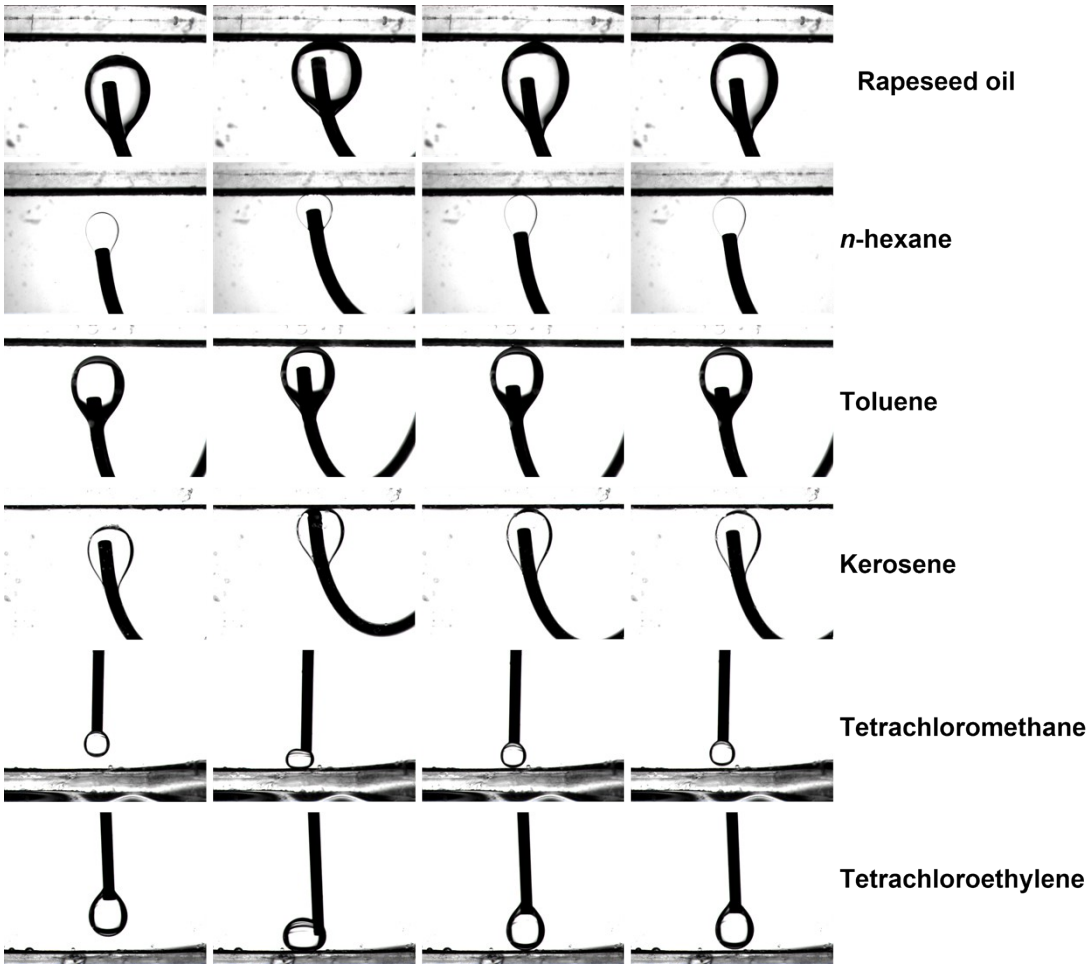

Fig. S9. The dynamic anti-oil adhesion images of the $Ti_3C_2Cl_2$-$(CuSA)_5$ membrane.

When the oil droplet thoroughly contacted the $Ti_3C_2Cl_2$-$(CuSA)_5$ membrane surface and subsequently moved away, there was no difference in its shape by comparing the shape of the oil droplet at the moment of leaving.

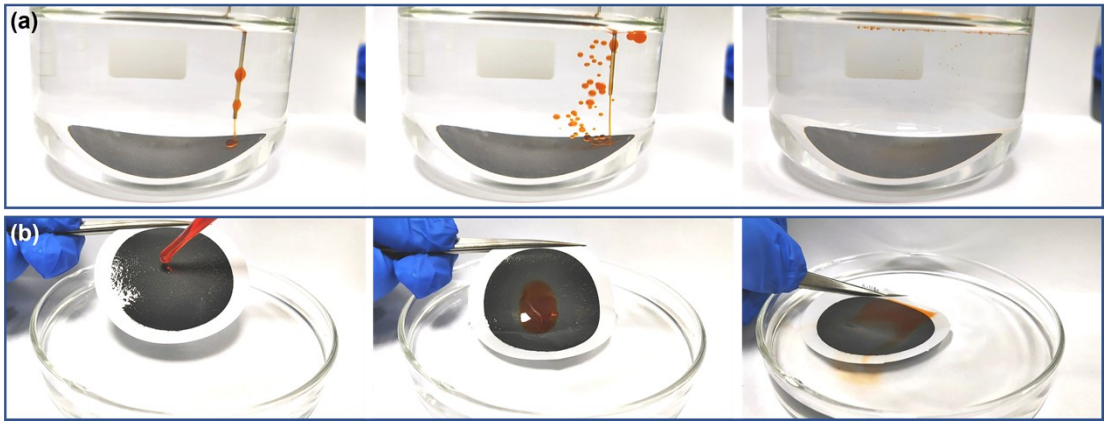

Fig. S10. (a, b) Dynamic anti-oil adhesion images of the $Ti_3C_2Cl_2$-$(CuSA)_5$ membrane. The test oil phases were (a) kerosene and (b) rapeseed oil, respectively, stained by Sudan II.

Underwater, many oil droplets were sprayed onto the $Ti_3C_2Cl_2$-$(CuSA)_5$ membrane surface, the oil droplets were bounced off and float upwards, and eventually no oil droplets sticked to the its surface (Fig. S10 and Video S1, S2). Meanwhile, a drop of oil was applied to the wetted membrane surface and subsequently placed in the water, when entering the water, the oil naturally floated up and there was no residual oil on its surface. These dynamic oil resistance results indicated that the strong hydration layer built by the hydrogel on the $Ti_3C_2Cl_2$-$(CuSA)_5$ membrane surface blocked the oil droplets from contacting the substrate.

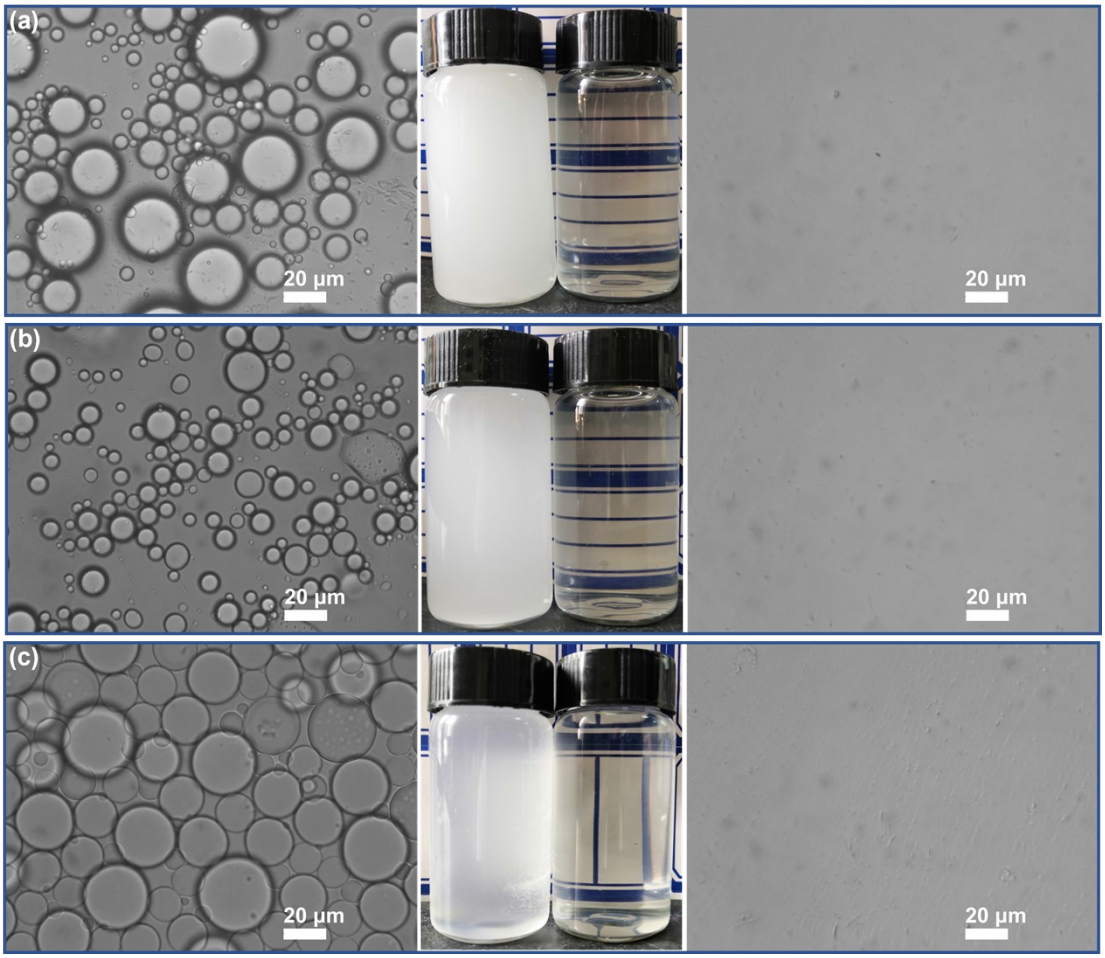

Fig. S11. Optical microscope photographs and digital photographs of the (a) rapeseed oil, (b) kerosene, and (c) *n*-hexane SDS-stabilized oil-in-water emulsions and their filtrates separated by the $Ti_3C_2Cl_2$-$(CuSA)_5$ membrane.

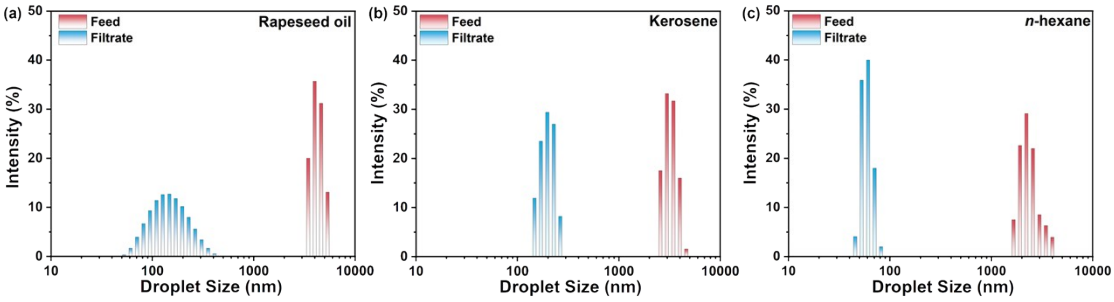

Fig. S12. The particle size distributions of the (a) rapeseed oil, (b) kerosene, and (c) *n*-hexane SDS-stabilized oil-in-water emulsions and their filtrates separated by the $Ti_3C_2Cl_2$-$(CuSA)_5$ membrane. The particle sizes of rapeseed oil, kerosene, and *n*-hexane emulsions were 3580-5560, 2670-4880, and 1720-4150 nm, respectively; after separation their filtrates were 50.7-459, 142-220, and 43.8-78.8 nm, respectively. The presence of the DLS particle size signals in the filtrate can be attributed to either micelles formed by residual SDS aggregates in the filtrate or residual oil droplets[3, 4].

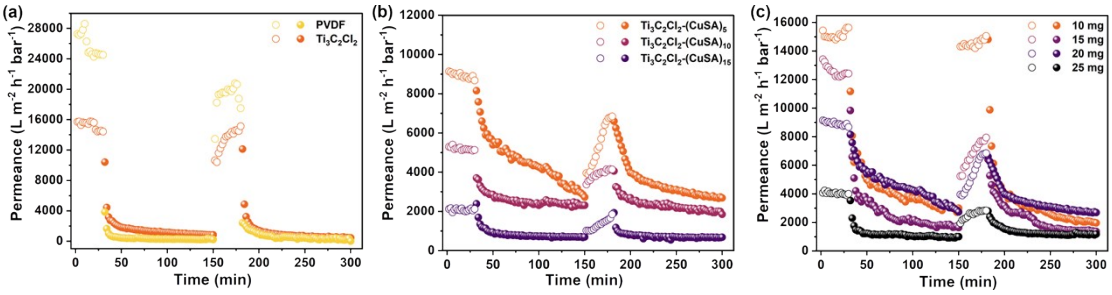

Fig. S13. (a) Real-time separation permeance of the PVDF and $Ti_3C_2Cl_2$ membranes when separating the *n*-hexane SDS-stabilized oil-in-water emulsion. (b) Real-time separation permeance of the $Ti_3C_2Cl_2$-$(CuSA)_5$, $Ti_3C_2Cl_2$-$(CuSA)_{10}$, and $Ti_3C_2Cl_2$-$(CuSA)_{15}$ membranes when separating the *n*-hexane SDS-stabilized oil-in-water emulsion. (c) Real-time separation permeance of the $Ti_3C_2Cl_2$-$(CuSA)_5$ membranes under different loading mass when separating the *n*-hexane SDS-stabilized oil-in-water emulsion. Hollow and solid spheres represent the water and emulsion permeance, respectively.

The PVDF and $Ti_3C_2Cl_2$ membranes showed similar permeance trends, both starting with a large water permeance and decreasing sharply with the separation of *n*-hexane emulsion; the water permeance was able to recover a little bit in the second cycle, but with the separation of *n*-hexane emulsion again, the permeance again decreased sharply, and tended to converge to the permeances of 16.7 and 439.5 L m^{-2} h^{-1} bar^{-1} for PVDF and $Ti_3C_2Cl_2$ membranes (Fig. S13a), respectively, after separating 300 min. This result can be attributed to them lacking anti-oil adhesion. The hydrogel layer wrapped around the $Ti_3C_2Cl_2$ outside was crucial in directly determining its separation performance, so it was indispensable to explore the number of times the hydrogel layer was constructed. As shown in Fig. S13b, as the number of hydrogel layer construction increased, both water and emulsion permeance showed a decreasing trend, and after separating 300 min, $Ti_3C_2Cl_2$-$(CuSA)_5$, $Ti_3C_2Cl_2$-$(CuSA)_{10}$, and $Ti_3C_2Cl_2$-$(CuSA)_{15}$ permeances were 2686.1, 1850.8, and 682.7 L m^{-2} h^{-1} bar^{-1}, respectively. Since the membrane was prepared by filtering the suspension onto the

substrate membrane, the loading mass of the sample affected its thickness and water transport path distance, which ultimately affected the membrane permeance. Additionally, insufficient sample loading may result in lacking anti-oil adhesion and affect the membrane separation permeance. Obviously, the water permeance decreased gradually with the loading mass increasing, and its emulsion separation permeance could maintain a high level when the loading mass was 20 mg; after separating 300 min, the membrane separation permeabilities with loading mass of 10,15,20, and 25 mg were 1958.7, 1358.8, 2686.1, and 1177.7 L m^{-2} h^{-1} bar^{-1}, respectively (Fig. S13c).

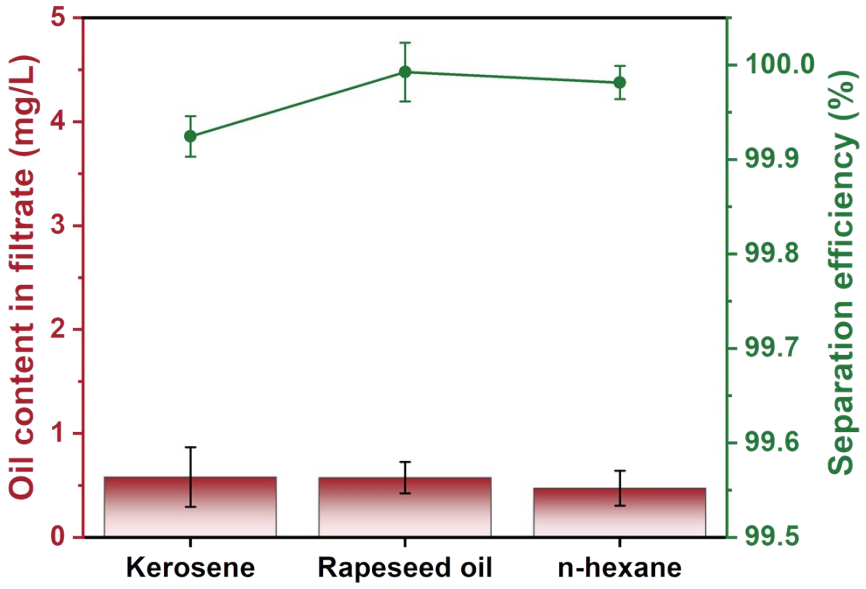

Fig. S14. Oil content in filtrate and separation efficiency of the $Ti_3C_2Cl_2$-$(CuSA)_5$ membrane when separating the kerosene, rapeseed oil, and *n*-hexane SDS-stabilized oil-in-water emulsions.

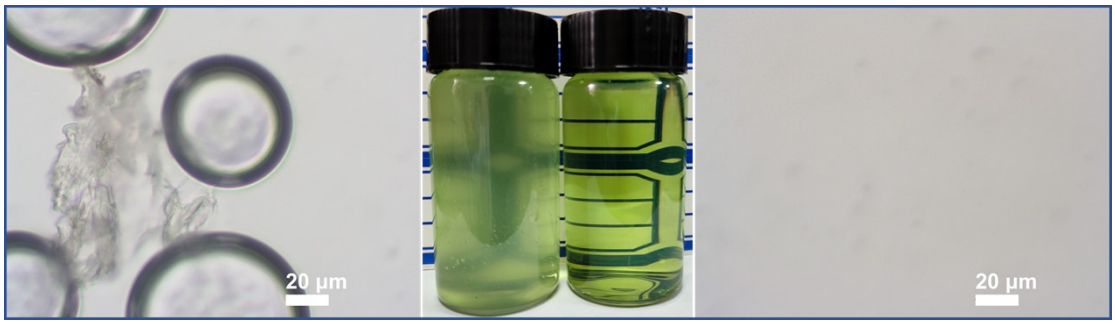

Fig. S15. Optical microscope photographs and digital photographs of the extract wastewater and its filtrate separated by the $Ti_3C_2Cl_2$-$(CuSA)_5$ membrane.

The extraction wastewater contained NaCl (97 g/L), $NiCl_2$ (12 g/L), $FeCl_3$ (9 g/L), sulfonated kerosene, octanol, and amine, pH was 0.13.

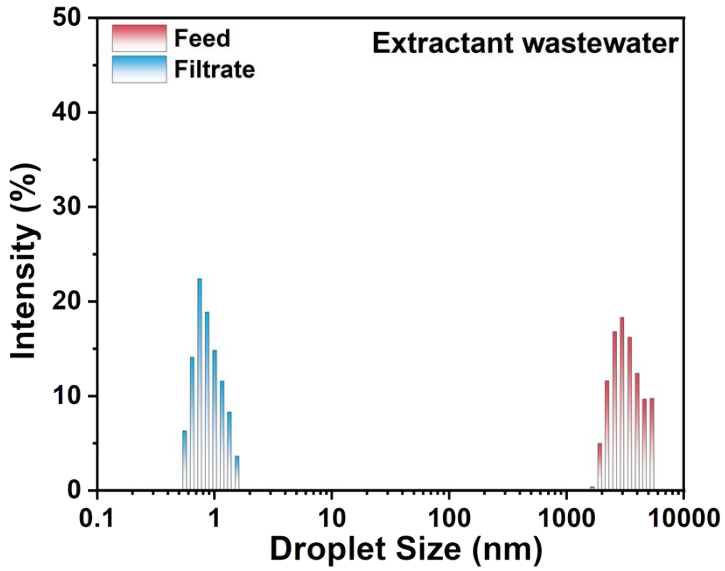

Fig. S16. particle size distributions of the extract wastewater and its filtrate separated by the $Ti_3C_2Cl_2$-$(CuSA)_5$ membrane.

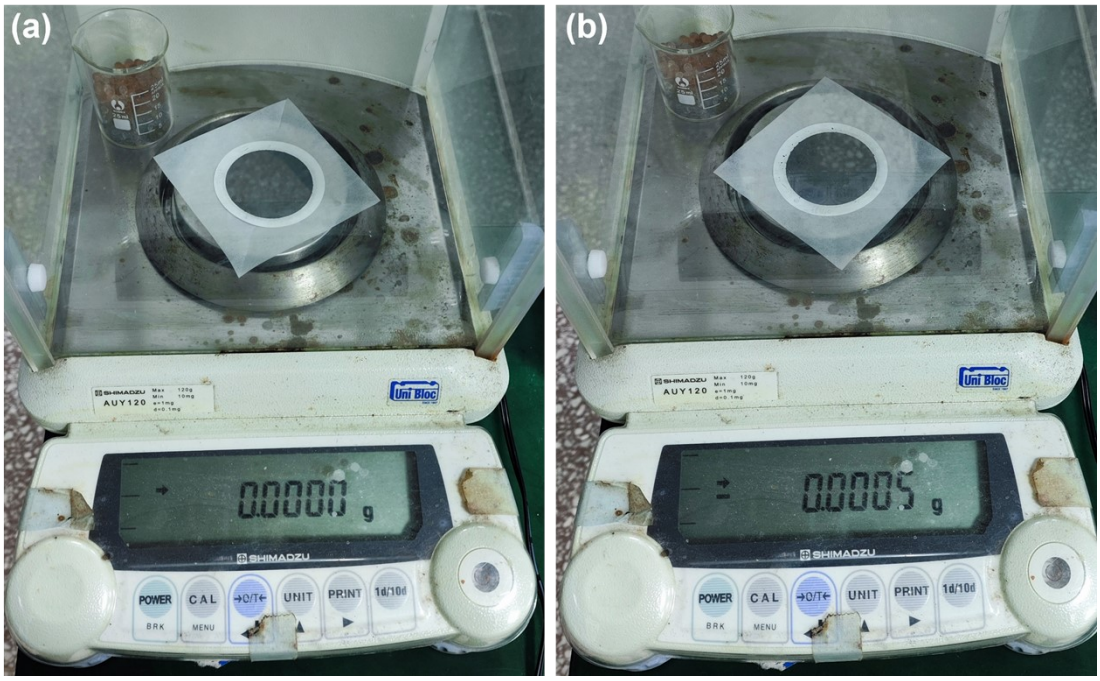

Fig. S17. Mass change of $Ti_3C_2Cl_2$-$(CuSA)_5$ membrane loaded with 20 mg (a) before and (b) after continuous 300 min separation.

After 300 min of continuous separation, only 0.5 mg of sample was lost from the $Ti_3C_2Cl_2$-$(CuSA)_5$ membrane, a sample loss of only 2.5%. There was little risk of sample dropout after long time separation, with the potential for long time and continuous separations.

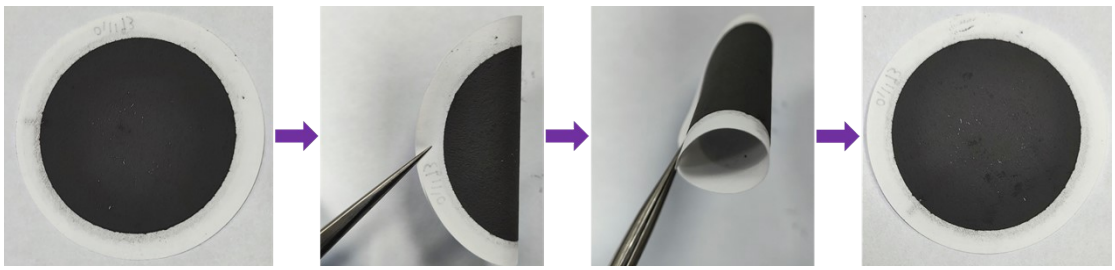

Fig. S18. The photograph of the $Ti_3C_2Cl_2$-$(CuSA)_5$ membrane after bending 200 times.

After the $Ti_3C_2Cl_2$-$(CuSA)_5$ membrane was continuously bent 200 times, none of the samples fell off, indicating that it exhibited a good bending performance and was suitable for installing membrane modules.

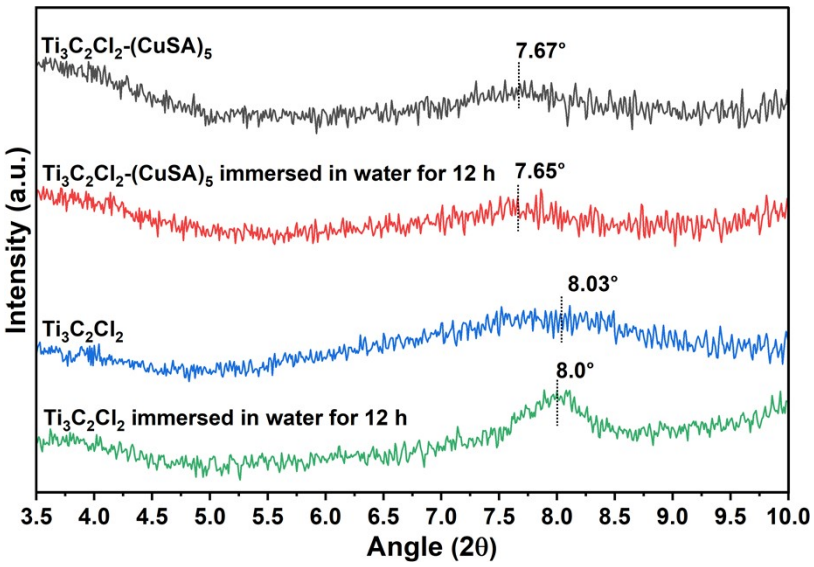

Fig. S19. XRD patterns of $Ti_3C_2Cl_2$, $Ti_3C_2Cl_2$-$(CuSA)_5$ membranes or they immersed in DI water for 12 h.

$Ti_3C_2Cl_2$, and $Ti_3C_2Cl_2$-$(CuSA)_5$ membranes after 12 h of immersion in DI water, their XRD results were not significantly different compared with that of the dry state. The (002) peaks for the $Ti_3C_2Cl_2$-$(CuSA)_5$ membrane were 7.67 and 7.65° in the dry and wet states, respectively, while the $Ti_3C_2Cl_2$ membrane was 8.03 and 8.0°. There was a slight and minor increased in layer spacing after the soaking treatment. The relative negative shift in the position of the (002) peak and the weaker peak intensity of the $Ti_3C_2Cl_2$-$(CuSA)_5$ membrane compared with that of the $Ti_3C_2Cl_2$ may be due to the multiple sonication and encapsulation of the hydrogel layer during the preparation of the $Ti_3C_2Cl_2$-$(CuSA)_5$ suspension. In addition, the hydrogel layer can slightly act as an anti-swelling of $Ti_3C_2Cl_2$-$(CuSA)_5$ membrane.

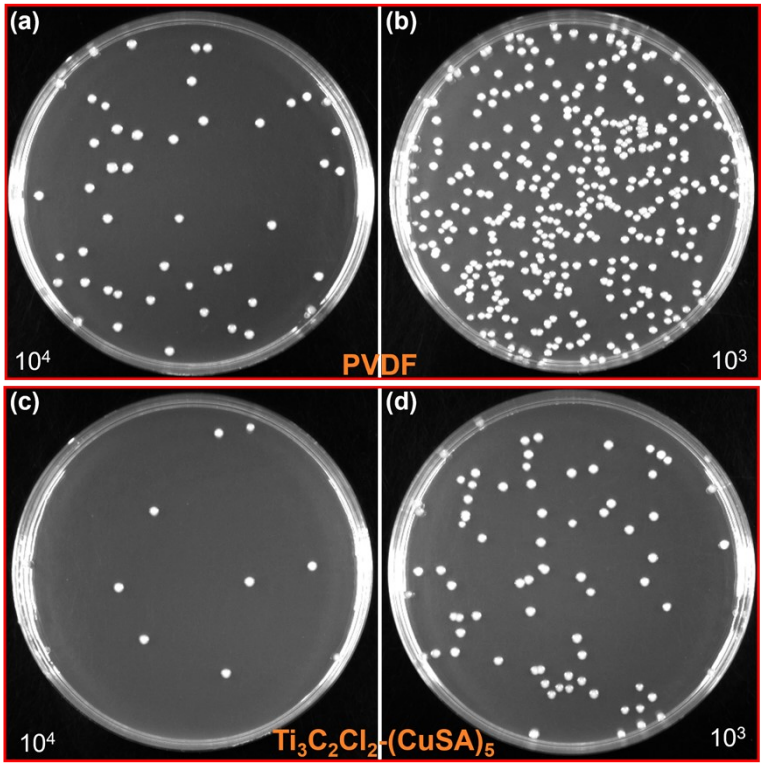

Fig. S20. Digital photographs of antimicrobial results of (a, b) PVDF and (c, d) $Ti_3C_2Cl_2$-$(CuSA)_5$ membrane groups. 10^4 and 10^3 represent colonies cultured at 10^4 and 10^3 dilutions, respectively.

Table S1. Performance of the MXene-based membranes.

Materials	Emulsions & water/oil mixture (ratio & volume)	Permeance (efficiency & cycles/time)	Pressure (bar)	Etching agent	Advantages
Ag-Bi_2O_3@MXene/PAN[5]	oily emulsion	2880[a] (99.51%, 10 cycles)	0.4	LiF/HCl	Antibacterial, dye adsorption
LDF-2-M[6]	Emulsion (1:99)	1862.0[a] (99.12%, 10 cycles)	/	LiF/HCl	Dye adsorption
MX-PAN[7]	Emulsion and mixture (1:9)	1573[a] (98.6%, 20 cycles), ~7000[a]	0	HF	Dye adsorption
M-APTES-PMA[8]	Emulsion (1:99, 100 mL)	6731.8[b] (99.97%, 10 cycles)	0.1	LiF/HCl	Heavy metals removal
PEG/MXene@MOF[9]	Emulsion (1:50, 50 mL)	1246 [b] (99.7%, 10 cycles/60 min)	0.8	LiF/HCl	Mechanical robustness
PMT[10]	Emulsion (1:100)	578.7[b] (99.9%, 10 cycles/300 min)	/	LiF/HCl	Photocatalytic self-cleaning
$Ti_3C_2T_x$ MXene[11]	Emulsion (1:100)	887[b] (99.4%, 10 cycles)	/	HF	/
This work	Emulsion (1:100)	2686.1[b] (99.99%, 300 min)	0.1	$CuCl_2$	Antibacterial

[a] represents L m^{-2} h^{-1}; [b] represents L m^{-2} h^{-1} bar^{-1}.

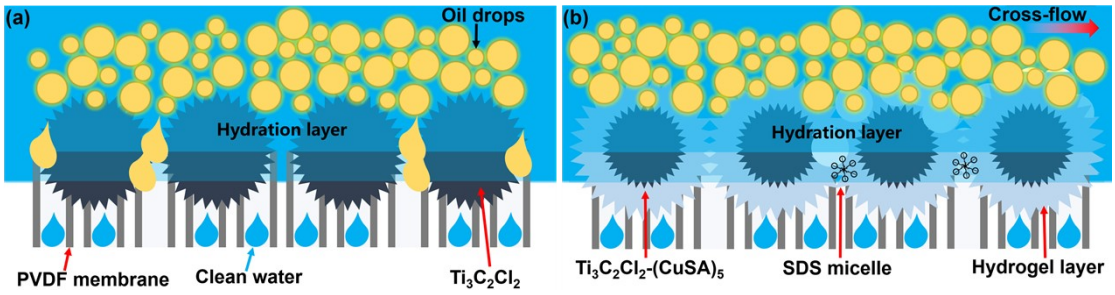

Fig. S21. Schematic diagram of the emulsion separation by (a) $Ti_3C_2Cl_2$ and (b) $Ti_3C_2Cl_2$-$(CuSA)_5$ membrane under a cross-flow device.

1. P. Huang and W.-Q. Han, *Nano-Micro Lett.*, 2023, **15**, 68.
2. Y. Zheng, X. Long, K. Han, W. Luo and F. Jiao, *Chem. Eng. Sci.*, 2024, **285**, 119580.
3. B. Liang, G. Zhang, Z. Zhong, T. Sato, A. Hozumi and Z. Su, *Chem. Eng. J.*, 2019, **362**, 126-135.
4. Y.-Q. Hu, H.-N. Li and Z.-K. Xu, *J. Membr. Sci.*, 2022, **648**, 120388.
5. Y. Zhan, X. Chen, A. Sun, H. Jia, Y. Liu, L. Li, Y.-H. Chiao, X. Yang and F. Zhu, *J. Hazard. Mater.*, 2023, **458**, 131965.
6. S.-y. Chen, Y.-f. Deng, T. Huang, N. Zhang and Y. Wang, *Sep. Purif. Technol.*, 2024, **328**, 125040.
7. R. Imsong and D. Dhar Purkayastha, *Sep. Purif. Technol.*, 2023, **306**, 122636.
8. X. Long, G.-Q. Zhao, Y. Zheng, J. Hu, Y. Zuo, W. Luo and F. Jiao, *Chem. Eng. J.*, 2023, **472**, 144904.
9. B. Xiang, J. Gong, Y. Sun, W. Yan, R. Jin and J. Li, *J. Membr. Sci.*, 2024, **691**, 122247.
10. Q. Zeng, D. L. Zhao, L. Shen, H. Lin, N. Kong, L. Han, C. Chen, J. Teng, C. Tang and T.-S. Chung, *Chem. Eng. J.*, 2023, **474**, 145579.
11. H. Zhang, Z. Wang, Y. Shen, P. Mu, Q. Wang and J. Li, *J. Colloid Interface Sci.*, 2020, **561**,

861-869.